Strain-induced valence-subband splitting in III-V semiconductors

M. Silver, W. Batty, A. Ghiti, and E. P. O'Reilly
University of Surrey, Guildford Surrey, GU2 5XH, England
(Received 26 February 1992)

A ⟨001⟩ axial strain introduces an additional term, known as the C_4 matrix element, into the valence-band Hamiltonian of III-V semiconductors, proportional to the axial strain and to $k_\perp$, the wave-vector component perpendicular to the strain axis. This matrix element has been ignored in all previous valence-subband calculations. We use the empirical pseudopotential method and the tight-binding method to calculate the magnitude of C_4 in the III-V and selected II-VI semiconductors. The calculated values are smaller than but comparable to the experimentally determined value in InSb. We then present envelope-function calculations which show how the C_4 term may particularly affect the valence-subband structure of quantum wells under biaxial tension (e.g., Ga-rich $In_xGa_{1-x}As$ on InP), splitting the degeneracy of the highest valence subband, and shifting the valence-band maximum from the Brillouin-zone center. The strain-induced band splittings are an order of magnitude larger than those in unstrained bulk material and may be measurable in wells with moderate strain (lattice mismatch $\approx 1\%$). Finally, we discuss the influence of the C_4 term on optical, transport, and cyclotron-resonance data.

I. INTRODUCTION

The band structure of a bulk tetrahedrally bonded group-IV semiconductor, such as Si, is doubly degenerate because of the inversion symmetry about the center of a Si-Si bond. By contrast, in a III-V zinc-blende semiconductor such as GaAs, the lack of inversion symmetry lifts this degeneracy, and introduces terms linear in wave vector k into the $\mathbf{k}\cdot\mathbf{p}$ Hamiltonian describing the band structure. These linear-k terms have been shown to be small in unstrained semiconductors[1,2] and so can be generally disregarded in band-structure calculations for both bulk and quantum-well systems.[3] The application of axial strain ε_{ax} in a III-V semiconductor further reduces the crystal symmetry, and introduces additional linear-k matrix elements into the valence-band Hamiltonian, proportional to ε_{ax} and to $k_\perp$, the wave-vector component perpendicular to the strain axis. We focus in this paper on the modifications to the valence-band structure when axial strain is applied along the [001] direction, appropriate to the case of growing strained-layer semiconductor structures on substrates with the conventional [001] alignment. We use both the empirical pseudopotential method and the tight-binding method to calculate the band structure and relevant momentum matrix elements for the bulk III-V semiconductors under a ⟨001⟩ axial strain. This strain introduces an additional matrix element, known as the C_4 term, to the valence-band Hamiltonian. We find that for a 1% lattice mismatch, the strain-induced linear-k terms are almost an order of magnitude larger than those associated with inversion asymmetry.

Strains of this magnitude are now routinely incorporated into strained-layer semiconductor structures,[4] but the influence of the C_4 matrix element has been ignored in all previous studies of strained-layer quantum-well structures. We include the C_4 term here and calculate the valence-subband structure of strained $In_xGa_{1-x}As$ quantum wells between unstrained InP barriers, for the case both of quantum-well layers under biaxial compression (In rich) and under biaxial tension (Ga rich). The additional term has little effect on the subband structure near the valence-band maximum of layers under biaxial compression, but can significantly affect the valence-subband structure of quantum wells under biaxial tension (here Ga-rich $In_xGa_{1-x}As$ on InP), splitting the degeneracy of the highest valence subband, and in all cases shifting the valence-band maximum from the Brillouin-zone center. We conclude that the strain-induced linear-k terms should be included when studying the valence-subband structure of quantum wells under biaxial tension but can be ignored in most applications for wells under biaxial compression.

We begin in the next section by discussing the valence-band structure of III-V semiconductors, using the Luttinger-Kohn (LK) Hamiltonian[5,6] in the spin-$\frac{3}{2}$ basis to describe the heavy- and light-hole bands. We describe how the LK Hamiltonian is modified by a ⟨001⟩ axial strain, including the incorporation of the C_4-related linear-k terms.[6] We use the empirical pseudopotential method[7] in Sec. III to calculate the value of the C_4 matrix element for each of the III-V semiconductors, and find it to be consistently smaller than but comparable to the experimentally determined value in InSb. Similar values are obtained in Sec. IV using Harrison's linear combination of atomic orbitals (LCAO) method.[8] We then take an estimated value of C_4 and use the envelope-function method in Sec. V to calculate the valence-subband structure of $In_xGa_{1-x}As$ quantum wells between InP barriers for layers under biaxial tension ($x < 0.53$) and biaxial compression ($x > 0.53$). Finally, we discuss our results and summarize our conclusions in Sec. VI.

II. VALENCE-BAND STRUCTURE

The application of an axial strain along the [001] direction breaks the cubic symmetry of a III-V semiconductor, distorting the unit cell as $(1+\varepsilon_\perp, 1+\varepsilon_\perp, 1+\varepsilon_\parallel)$ and thereby modifying the band structure. The total strain can be resolved into a purely axial component

$$\varepsilon_{ax}=\varepsilon_\parallel-\varepsilon_\perp \tag{2.1}$$

and a hydrostatic component

$$\varepsilon_{vol}=\varepsilon_\parallel+2\varepsilon_\perp\ . \tag{2.2}$$

We are primarily interested in the effects of the axial strain ε_{ax} but will also, where appropriate, consider the effects of the hydrostatic strain ε_{vol}.

The valence-band structure of unstrained GaAs, taken as the prototype III-V semiconductor, is shown in Fig. 1(a), calculated using the empirical pseudopotential method, as described in the next section. Figures 1(b) and 1(c) show the band structure with net positive ($\varepsilon_{ax}=-3\%$) and negative ($\varepsilon_{ax}=3\%$) axial strains, respectively. For both calculations, $\varepsilon_\parallel=-2\varepsilon_\perp$, so that $\varepsilon_{vol}=0$. The band structure is plotted along the strain direction, $\Delta_\parallel$ [001], and perpendicular to it, along $\Delta_\perp$ [100], and extends 20% into the Brillouin zone. In each case, the lowest conduction band is approximately parabolic near the zone center. The description of the holes is complicated even in the unstrained case [Fig. 1(a)]. The heavy-hold (HH) and light-hole (LH) bands are degenerate at the zone center Γ, and the spin-split-off (SO) band lies at an energy Δ_0 below the two highest bands. The application of axial strain has three noticeable effects on the band structures of Figs. 1(b) and 1(c). First, it splits the degeneracy of the light- and heavy-hole states at Γ, typically by about 100 meV for $\varepsilon_{ax}=3\%$. Secondly, it introduces an anisotropic valence-band structure, with the band that is heavy along the [001] direction, $k_\parallel$, being comparatively light perpendicular to that direction, along $k_\perp$, and vice versa. Finally, axial strain splits the degeneracy of the spin-up and spin-down valence states along $k_\perp$, away from the strain axis. The band splitting increases linearly with wave vector $k_\perp$ for the highest valence band in Fig. 1(c), and this in fact results in a slight shift in the valence-band maximum away from Γ ($k=0$) in this case.

The strain-induced splitting of the heavy and light valence-band-maximum states, and consequent anisotropic band structure, have been widely discussed in relation to strained-layer quantum-well structures,[4] where they have been shown to lead to a reduced hole mass in layers under biaxial compression, with consequent benefits for laser applications. Little attention has been paid to the strain-induced band splitting of the spin-up and spin-down states, on which we now focus.

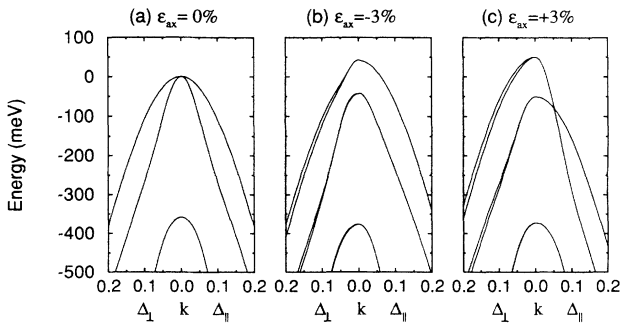

FIG. 1. Valence-band structure of GaAs for (a) unstrained, (b) biaxial compression ($\varepsilon_{ax}=-3\%$), and (c) biaxial tension ($\varepsilon_{ax}=+3\%$). The strain is applied along the (001) direction, and band dispersions are shown 20% into the Brillouin zone. The (100) direction ($\Delta_\perp$) is then perpendicular, and the (001) ($\Delta_\parallel$) parallel to the strain axis. Along the direction perpendicular to the strain axis ($\Delta_\perp$), the strain-induced matrix element C_4 splits the degeneracy of the spin states by a sizable amount, even for moderate strains. The effect of C_4 on the highest valence band will therefore be greater in strain-layer systems under tension (c) than for layers under compression (b).

We describe the valence-band structure in the vicinity of the band maximum using the Luttinger-Kohn Hamiltonian in the spin-$\frac{3}{2}$ basis, with the axis of quantization taken along the (001) direction. The most general form of the LK Hamiltonian for an unstrained III-V semiconductor in zero magnetic field is[5]

$$\begin{aligned}H=-\frac{\hbar^2}{2m}&(\gamma_1 k^2 I-2\gamma_2[(J_x^2-\tfrac{1}{3}J^2)k_x^2+\text{c.p.}]\\&-4\gamma_3[\{J_xJ_y\}k_xk_y+\text{c.p.}])\\&+\frac{2C}{\sqrt{3}}[\{J_x(J_y^2-J_z^2)\}k_x+\text{c.p.}]\ ,\end{aligned} \tag{2.3}$$

where I is the (4×4) unit matrix, J_x, J_y, and J_z are the angular momentum matrices for spin $\frac{3}{2}$, and x, y, and z denote the crystallographic [001] directions. $\{J_xJ_y\}=\frac{1}{2}(J_xJ_y+J_yJ_x)$, and c.p. stands for cyclic permutation of the preceding term. Equation (2.3) can be rewritten as

$$H=\begin{array}{c}\\ \frac{3}{2}\\ \frac{1}{2}\\ -\frac{1}{2}\\ -\frac{3}{2}\end{array}\begin{array}{c}\begin{array}{cccc}\quad\frac{3}{2}\quad & \quad\frac{1}{2}\quad & \quad-\frac{1}{2}\quad & \quad-\frac{3}{2}\quad\end{array}\\ \begin{bmatrix} a_+ & b+d'^*/\sqrt{3} & c-d & d' \\ b^*+d'/\sqrt{3} & a_- & -d'^* & c+d \\ c^*-d & -d' & a_- & -b+d'^*/\sqrt{3} \\ d'^* & c^*-d & -b^*+d'/\sqrt{3} & a_+ \end{bmatrix}\end{array}, \tag{2.4}$$

where

$$a_{\pm}=-\tfrac{1}{2}(\gamma_1\mp 2\gamma_2)k_z^2-\tfrac{1}{2}(\gamma_1\pm\gamma_2)(k_x^2+k_y^2)\ ,$$
$$b=i\sqrt{3}\gamma_3(k_x-ik_y)k_z\ ,$$
$$c=-\sqrt{3}[\gamma_2(k_x^2-k_y^2)-2i\gamma_3 k_x k_y]/2\ ,$$
$$d=Ck_z\ ,$$
$$d'=i\sqrt{3}C(k_x-ik_y)/2\ .$$

We have taken $\hbar=m=1$ in Eq. (2.4). The $m_J=\pm\frac{3}{2}$ states correspond to the heavy-hole bands and the $m_J=\pm\frac{1}{2}$ states to the light-hole bands along (001), with the heavy-hole mass then given by $m_h^*=(\gamma_1-2\gamma_2)^{-1}$ and the light-hole mass by $m_l^*=(\gamma_1+2\gamma_2)^{-1}$. The linear-$k$ terms arise from the lack of inversion symmetry in III-V semiconductors, but are generally considered to be very small. Brillouin scattering experiments were unable to detect any linear-k splittings in GaAs,[9] while theoretical calculations have estimated a value for C in GaAs of 3.4 meV Å.[2] Experimentally determined values of C in other zinc-blende semiconductors vary between 9.3 meV Å (InSb) and 20.0 meV Å (CdTe).[2] These C terms are therefore small and can be ignored in valence-band calculations.

The application of an axial strain along the (001) direction further reduces the symmetry and introduces additional terms H_ε into the LK valence-band Hamiltonian, with the terms up to εk being given by[5]

$$H_\varepsilon=a_v\varepsilon_{\rm vol}I-b[(J_x^2-\tfrac{1}{3}J^2)\varepsilon_{xx}+\text{c.p.}]$$
$$+[J_xC_4(\varepsilon_{yy}-\varepsilon_{zz})k_x+\text{c.p.}]\ , \qquad (2.5)$$

where a_v and b are the valence-band volume and axial deformation potentials, $\varepsilon_{xx}=\varepsilon_{yy}=\varepsilon_\perp$, $\varepsilon_{zz}=\varepsilon_\parallel$, while C_4 describes the strain-induced linear-k splittings. Equation (2.5) can be rewritten as

$$H_\varepsilon=\begin{matrix}\frac{3}{2}\\ \frac{1}{2}\\ -\frac{1}{2}\\ -\frac{3}{2}\end{matrix}\begin{Bmatrix} S & \sqrt{3}/2f & 0 & 0\\ \sqrt{3}/2f^* & -S & f & 0\\ 0 & f^* & -S & \sqrt{3}/2f\\ 0 & 0 & \sqrt{3}/2f^* & S\end{Bmatrix}, \qquad (2.6)$$

where $S=-b\varepsilon_{\rm ax}$, $f=-iC_4\varepsilon_{\rm ax}(k_x-ik_y)$, and we have set $a_v\varepsilon_{\rm vol}=0$. The strain-induced splitting of the valence-band maximum in Figs. 1(b) and 1(c) are then described by the diagonal terms in Eq. (2.6), and the band splittings away from the (001) axial strain direction by the off-diagonal terms in Eq. (2.6).

C_4 has been defined by Trebin[5] using perturbation theory in terms of the unstrained basis states as

$$iC_4=\frac{2}{3}\frac{\hbar}{m}\times\sum_j^{\Gamma_4,\Gamma_5}\frac{\langle X|p_y|j\rangle\langle j|D_{zz}|Z\rangle+\langle X|D_{zz}|j\rangle\langle j|p_y|Z\rangle}{E_v-E_j}\ , \qquad (2.7)$$

where

$$D_{zz}=\frac{-p_z^2}{m}+\frac{\partial V}{\partial\varepsilon_{zz}}\ .$$

In our pseudopotential and LCAO methods described below, we calculate C_4 directly from the strained basis states.

III. PSEUDOPOTENTIAL METHOD AND RESULTS

In this section, we use the empirical pseudopotential method (EPM) with the local approximation to calculate the magnitude of the C_4 matrix element for the III-V semiconductors. We use published values of the form factors[7,10–14] to calculate the band structure of the unstrained bulk semiconductors. We then determine how the form factors vary with axial strain to reproduce experimentally measured deformation potentials. The strain-dependent form factors are finally used to calculate the relevant matrix element. The eigenvalues and eigenvectors are calculated in each case by diagonalizing a 113×113 plane-wave matrix (doubling in size when spin is included), which ensures energy convergence to within 0.01 eV.

The variation in band structure with $\varepsilon_{\rm ax}$ was calculated by introducing a purely axial strain along the [001] direction, distorting the unit cell as $(1+\varepsilon,1+\varepsilon,1-2\varepsilon)$, so that $\varepsilon_{\rm ax}=3\varepsilon$, and, to first order, there is no change in volume. Keeping the volume constant ensures that the screening and form-factor normalization are unchanged, and consequently the strain-dependent band structure can be calculated once the gradient of the form factors at the relevant reciprocal-lattice vectors has been determined. In fact, only four of the six form-factor slopes need to be determined, since a $\langle 001\rangle$ axial strain has no effect on the symmetric form factor $V_S(q)$ and the antisymmetric form factor, $V_A(q)$ for $q^2=(2\pi/a)^2 3$, where q is the reciprocal space vector.

The empirical determination of the form-factor gradients was carried out in a two-stage process. First, a "best guess" was made of the gradients by polynomial fitting of the unstrained symmetric and antisymmetric form factors. The gradients were then modified using a numerical fitting technique to optimize the calculated values of the deformation potential b associated with the (001) axial-strain-induced splitting of the valence-band maximum, where the strain-induced splitting S between the $m_J=\frac{3}{2}$ and $\frac{1}{2}$ states is given by $S=2b\varepsilon_{\rm ax}$. We also monitored the splitting of the conduction-band X minima, where the separation between the $X_{x,y}$ and the X_z state is given by $E_2\varepsilon_{\rm ax}$; here E_2 is the relevant strain deformation potential.[15] An additional constraint was included in the fitting procedure to ensure that the calculated slopes remained close to those predicted by polynomial fitting. This process was repeated for all the group-IV and III-V semiconductors. The calculated values of b and E_2 are listed in Table I, along with the available experimental data. There is good agreement between theory and experiment.

TABLE I. Experimental and theoretical deformation potentials (in eV) for the main group-IV and III-V semiconductors. The sixth and seventh columns contain the calculated values of the intervalence-band momentum matrix element (C_4) in units of eV Å, from the EPM and LCAO methods, respectively. Also shown is the experimentally determined value for InSb (in italics).

Material	b_{calc} (eV)	b_{expt} (eV)	$E_{2\,\text{calc}}$ (eV)	$E_{2\,\text{expt}}$ (eV)	EPM C_4 (eV Å)	LCAO C_4 (eV Å)
Si	−2.1	−2.1	14.0	9.2	0.0	0.0
Ge	−2.4	−2.4	11.5	9.5	0.0	0.0
AlP	−1.5	−1.5	7.7		3.5	7.3
AlAs	−1.6	−1.5	7.1		4.3	6.9
AlSb	−1.4	−1.4	7.3	5.4	3.7	6.0
GaP	−1.5	−1.5	7.6	6.4	3.3	7.3
GaAs	−1.7	−1.7	7.8	6.3	3.2	6.8
GaSb	−1.9	−2.0	4.7		2.2	6.0
InP	−1.9	−2.0	6.5		2.3	7.4
InAs	−1.7	−1.8	3.7		2.9	7.0
InSb	−1.9	−2.0	2.8		2.0	6.3
					11.3 (expt.)	
ZnS	−0.8	−0.8	2.7		0.8	8.4
ZnSe	−1.2	−1.2	8.2		0.3	8.0
ZnTe	−1.0	−1.0	7.0		1.3	7.5
CdTe	−1.1	−1.1	2.5		0.6	6.9

The calculated values of the intravalence-band momentum matrix element C_4 are also shown in Table I, in units of eV Å. C_4 is zero for the group-IV materials due to the higher symmetry of the diamond lattice. The calculated values of C_4 are all comparable to but smaller than that derived from experiment for InSb, where C_4 was determined to be 11.3 eV Å.[16] We have carried out further calculations which indicate that the difference between the theoretical and experimental values cannot be removed by considering different form-factor sets, or sensible alternative values for the form-factor slopes. Rather, we would need to alter severely the form-factor slopes, beyond physical feasibility, to calculate a value of C_4 equal to the experimentally determined value in InSb. We thus conclude that the discrepancy between the one experimental value for C_4 and our results cannot be caused by the fitting procedure adopted.

IV. LCAO METHOD AND RESULTS

We use Harrison's tight-binding LCAO method[8] with an sp^3 basis to estimate the magnitude of C_4 in the III-V and selected II-VI semiconductors in this section.

The valence-band maximum is triply degenerate in a zinc-blende semiconductor when the spin-orbit interaction is ignored, and is of Γ_{15} symmetry. The three Γ_{15} states can be described by wave functions that are of x-, y-, and z-like symmetry, which we refer to as the $|X\rangle$, $|Y\rangle$, and $|Z\rangle$ states, respectively. The wave function of the $|X\rangle$ state is given in the LCAO sp^3 basis as

$$|X\rangle=\left[\frac{1+\alpha_p^x}{2}\right]^{1/2}|p_x^{\text{V}}\rangle-\left[\frac{1-\alpha_p^x}{2}\right]^{1/2}|p_x^{\text{III}}\rangle$$
$$=a_x|p_x^{\text{V}}\rangle-c_x|p_x^{\text{III}}\rangle\ , \tag{4.1}$$

with similar expressions for the $|Y\rangle$ and $|Z\rangle$ states. In the above equation, $|p_x^{\text{V (III)}}\rangle$ describes a p state on the group-V (group-III) site and α_p^x is the ionicity of the $|X\rangle$ state, defined by

$$\alpha_p^x=\frac{\frac{1}{2}(\varepsilon_p^{\text{III}}-\varepsilon_p^{\text{V}})}{[\frac{1}{4}(\varepsilon_p^{\text{III}}-\varepsilon_p^{\text{V}})^2+(4V_{xx})^2]^{1/2}}\ , \tag{4.2}$$

where $\varepsilon_p^{\text{V (III)}}$ is the self-energy of a p atomic orbital on the group-V (group-III) site, and V_{xx} describes the covalent interaction between $|p_x\rangle$ states on neighboring sites, given by

$$V_{xx}=l^2(V_{pp\sigma}-V_{pp\pi})+V_{pp\pi}\ , \tag{4.3}$$

where $(l,m,n)=(1/\sqrt{3})(1,1,1)$ is the direction cosine between neighboring sites and $V_{pp\sigma}$ and $V_{pp\pi}$ are the interatomic matrix elements between p states pointing, respectively, parallel and perpendicular to the bond direction. The Hamiltonian interaction between the $|Y\rangle$ and $|Z\rangle$ states is zero in an unstrained crystal for a wave vector k_x along the (100) direction, because the y and z directions are equivalent, and so

$$\langle Y|H(k_x)|Z\rangle=\begin{cases}4iV_{xy}\sin(k_xa/4)(c_ya_z-a_yc_z)\\ 0\ \text{ when }\alpha_p^y=\alpha_p^z\ ,\end{cases} \tag{4.4}$$

where V_{xy} in Eq. (4.4) describes the interaction between a $|p_i\rangle$ and $|p_j\rangle$ state on neighboring sites ($i\neq j$) and is given in the present case by

$$V_{xy}=mn(V_{pp\sigma}-V_{pp\pi})\ . \tag{4.5}$$

Application of a purely axial (001) strain modifies the direction cosines as $(1/\sqrt{3})(1+\varepsilon,1+\varepsilon,1-2\varepsilon)$, with $\varepsilon_{\text{ax}}=3\varepsilon$. This strain changes the symmetry of the z direction relative to the x and y directions, so that α_p^y no longer equals α_p^z and we find, for small k_x, that

$$\langle Y|H(k_x)|Z\rangle = -i\frac{(V_{xy})^2}{V_{xx}}\alpha_p\alpha_c k_x a\varepsilon_{ax} , \tag{4.6}$$

where $\alpha_c=(1-\alpha_p^2)^{1/2}$ and a is the lattice constant. We take the values of V_{xx} and V_{xy} from Harrison's solid-state table, where they are both proportional to a^{-2}, and find that C_4 is then given by

$$C_4=\frac{2}{3}\frac{(V_{xy})^2}{V_{xx}}\alpha_p\alpha_c a=12\frac{\hbar^2}{ma}\alpha_p\alpha_c . \tag{4.7}$$

It can be seen, as expected, that C_4 is zero in a purely covalent material such as Si, where $\alpha_p=0$, and would also be zero in a purely ionic material, where $\alpha_c=0$. The calculated values of C_4 for the III-V semiconductors are shown in Table I, using values of α_p and α_c derived from the solid-state table.

The values of C_4 calculated using the LCAO method lie between the EPM values and the experimental value determined for InSb. We note that the calculated C_4 values for the selected II-VI compounds are larger than those for the III-V compounds in the LCAO method but are significantly smaller in the EPM calculation. We believe that this discrepancy can be understood using Eq. (4.7), which predicts that C_4 equals zero in the purely covalent ($\alpha_p=0$) or purely ionic compound ($\alpha_c=0$) and is maximized when $\alpha_p=\alpha_c=0.707$. In the LCAO calculations, the III-V compounds are weakly ionic ($\alpha_p\approx0.5$), while the II-VI compounds are more ionic, with $\alpha_p\approx0.7$. Thus C_4 increases in going from the III-V to II-VI compounds in the LCAO case. We have not derived an expression analogous to Eq. (4.7), but presume that the same trend holds with varying ionicity, except that now the III-V compounds have ionicities closer to that which gives the peak value of C_4, with the selected II-VI compounds having ionicities well beyond the C_4 peak.

If we regard a typical EPM value of 2.5 eV Å as a lower estimate of C_4 and the experimental value of 11.3 eV Å as an upper estimate, then for a value of axial strain of $\varepsilon_{ax}=3\%$, we find $C_4\varepsilon_{ax}\approx75-350$ meV Å, so that the strain-induced linear-k terms in Eq. (2.6) are approximately an order of magnitude larger than the linear-k terms due to inversion asymmetry in Eq. (2.4). We now turn to consider in the next section the influence of the C_4-related terms on the valence-subband structure of typical quantum-well structures with built-in axial strain.

V. BAND-STRUCTURE CALCULATIONS

It is now possible to grow high-quality strained-layer quantum-well structures, in which the quantum well is composed of a semiconductor which would normally have a significantly different lattice constant from the substrate. For GaAs/$In_xGa_{1-x}As$, which is the most widely studied III-V system, high-quality growth is now routinely achieved in structures where the product of lattice-mismatch ε_0 and well width L_z is of order 200 Å%. The lattice constant of $In_xGa_{1-x}As$ is greater than GaAs, so that strained $In_xGa_{1-x}As$ quantum wells on a GaAs substrate are always under biaxial compression. By contrast, the lattice constant of InP lies between that of InAs and GaAs, so that it is possible to grow $In_xGa_{1-x}As$ quantum wells on InP which are under either biaxial tension ($x<0.53$) or biaxial compression ($x>0.53$).[17,18] We have therefore chosen $In_xGa_{1-x}As$ quantum wells between InP barriers as the prototype system in which to consider the influence of strain-induced valence-band splittings.

The valence-subband structure is calculated using the envelope-function method[19] with the Hamiltonian of Eqs. (2.4) and (2.6), but ignoring the linear-k terms present due to inversion asymmetry in Eq. (2.4). The Luttinger γ parameters are shown in Table II. The InP γ parameters were taken from Lawaetz,[20] while the $In_xGa_{1-x}As$ values were obtained by linear interpolation of effective masses between unstrained bulk GaAs (Ref. 21) and InAs,[15] but allowing via the $\mathbf{k}\cdot\mathbf{p}$ interaction for the variation in the light-hole mass with strain in the quantum well. The axial deformation potential b was assumed to vary linearly between the GaAs and InAs values, and the built-in axial strain ε_{ax} was related to the lattice mismatch ε_0 as

$$\varepsilon_{ax}=-\frac{1+\sigma}{1-\sigma}\varepsilon_0 , \tag{5.1}$$

where σ is Poisson's ratio, taken equal to $\frac{1}{3}$ across the alloy system. The band offsets were then calculated using Van de Walle's model-solid theory.[22] We also list the C_4 values used in our calculations.

Figure 2 shows the calculated valence-subband dispersion in the quantum-well plane for (i) 50 Å and (ii) 100 Å $In_xGa_{1-x}As$ quantum wells on unstrained InP substrate which are (a) under biaxial compression ($x>0.53$), (b) unstrained ($x=0.53$) and (c),(d) under biaxial tension ($x<0.53$). The lifting of the spin degeneracy, particularly for layers under tension, is a direct result of C_4. The compositions are equivalent to a lattice mismatch of ε_0=(a) −1%, (b) 0%, (c) 1%, and (d) 2%, respectively, so that for all the structures considered $\varepsilon_0 L_z\leq200$ Å%, and lies within the range of good quality growth in the $In_xGa_{1-x}As$ system.

TABLE II. Material parameters used in valence-subband-structure calculations.

Material		γ_1	γ_2	γ_3	b (eV)	C_4 (eV Å)
InP		6.28	2.08	2.76	−2.00	3.45
$In_xGa_{1-x}As$	$\varepsilon_\perp=-1\%$	11.06	4.06	4.94	−1.77	4.52
	$\varepsilon_\perp=0\%$	9.80	3.43	4.29	−1.75	4.58
	$\varepsilon_\perp=1\%$	8.73	2.90	3.74	−1.74	4.65
	$\varepsilon_\perp=2\%$	7.90	2.48	3.30	−1.72	4.71

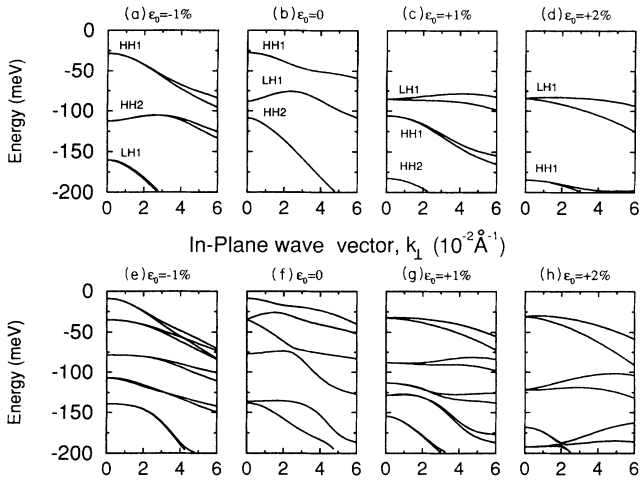

FIG. 2. In-plane valence-subband dispersions for (a)–(d) 50 Å and (e)–(h) 100 Å strained layers of $In_xGa_{1-x}As$ between unstrained InP barriers. For each well width four compositions are shown equivalent to the following lattice mismatches (a),(e) $\varepsilon_0=-1\%$; (b),(f) $\varepsilon_0=0\%$; (c),(g) $\varepsilon_0=1\%$; and (e),(h) $\varepsilon_0=2\%$. This encompasses layers under compression ($\varepsilon_0<0$), tension ($\varepsilon_0>0$), and unstrained ($\varepsilon_0=0$). The strain-induced splitting has the greatest effect on layers under tension, since $m_J=\pm\frac{1}{2}$ (light-hole) derived states are the highest valence states.

We see that the strain-induced splitting of the highest subband at the valence-band maximum is linear in k for layers under sufficient biaxial tension, [(c),(d)] but not for layers under biaxial compression. This follows immediately from the strain-dependent Hamiltonian of Eq. (2.6), where the off-diagonal linear-k terms cause a direct interaction between the otherwise degenerate light-hole ($\pm\frac{1}{2}$) states, while mixing the heavy-hole ($\pm\frac{3}{2}$) states with nondegenerate light-hole states, which causes the splitting to vary slowly near the zone center, as k^3. We thus conclude that the strain-induced C_4 terms can generally be ignored when considering carriers near the valence-band maximum in quantum wells under biaxial compression [Fig. 2(a)] but that they can have a significant influence on layers under biaxial tension [Figs. 2(c) and 2(d)], in particular shifting the valence-band maximum away from the Brillouin-zone center at Γ.

We seek to quantify the influence of the C_4 terms by considering the valence-band Hamiltonian in the decoupled approximation, where we ignore the interactions between heavy-hole ($m_J=\pm\frac{3}{2}$) and light-hole ($m_J=\pm\frac{1}{2}$) states. The Hamiltonian for the $m_J=\pm\frac{1}{2}$ states is then given by

$$H_{\mathrm{LH}}=\begin{matrix}+\frac{1}{2}\\-\frac{1}{2}\end{matrix}\begin{bmatrix} a_- -S & C_4\varepsilon_{ax}k_\perp e^{i\theta} \\ C_4\varepsilon_{ax}k_\perp e^{-i\theta} & a_- -S \end{bmatrix}, \tag{5.2}$$

where θ is the angle of $k_\perp$ in the x-y plane. The splitting Q for an in-plane wave vector of magnitude $k_\perp$ is then given by

$$Q=2C_4\varepsilon_{ax}k_\perp . \tag{5.3}$$

This leads to a splitting of 10 meV by $k_\perp=6\times10^{-2}$ Å^{-1} when $\varepsilon_{ax}=2\%$ [Fig. 2(c)], and of 19 meV for $\varepsilon_{ax}=4\%$ [Fig. 2(d)], where we assumed in the calculations that $C_4\approx4$ eV Å. The latter splitting would have been as large as 53 meV if we had assumed a value of 11 eV Å for C_4, equivalent to the experimentally determined value in InSb.[16] This would be a sizable distortion of the band structure, which would significantly modify the transport properties.

From Eq. (5.2), the highest $m_J=\pm\frac{1}{2}$ valence state will always be shifted from the zone center ($k_\perp=0$) by the C_4 terms, and the dispersion will vary near the zone center as

$$E(k_\perp)=E_{L1}-\frac{\hbar^2}{2m^*_{1/2}}k_\perp^2+C_4\varepsilon_{ax}k_\perp , \tag{5.4}$$

where E_{L1} is the energy of the highest $m_J=\pm\frac{1}{2}$ state at $k_\perp=0$ and $m^*_{1/2}$ is the in-plane effective mass when $C_4=0$. The band maximum will then occur at $k_\perp=m^*_{1/2}C_4\varepsilon_{ax}/\hbar^2$ and will be at an energy $\Delta E=\frac{1}{2}(C_4\varepsilon_{ax})^2m^*_{1/2}/\hbar^2$. This translates in the decoupled approximation [Eq. (5.2)] into a shift of 0.4 meV for $C_4\approx4$ eV Å and $\varepsilon_{ax}\approx2\%$, and a shift of 13 meV for $C_4\approx11$ eV Å and $\varepsilon_{ax}\approx4\%$. Here we have assumed an in-plane effective mass equal to the free-electron mass $m^*_{1/2}=m_0$, a typical value for tensile-strained quantum wells. A shift of the latter magnitude would again cause a significant distortion of the band structure.

Finally, we consider the influence of the C_4 terms on the Landau-level dispersion in a strained quantum-well structure under biaxial tension, using the decoupled approximation of Eq. (5.2), where we ignore interactions with the $m_J=\pm\frac{3}{2}$ states. For a magnetic field along the (001) direction, the Landau-level dispersion for the $m_J=\pm\frac{1}{2}$ states can be found for the 2×2 matrix (5.2) in an analogous way to that previously published.[3,23,24] It involves replacing the vector $\mathbf{k}$ in the valence-band Hamiltonian by $\mathbf{k}+e\mathbf{A}/\hbar$, where $\mathbf{A}$ is the vector potential, and by introducing a term of weight κ along the matrix diagonal.[5] For a field along the (001) direction the vector potential changes the valence-band Hamiltonian such that k_x and k_y are replaced by harmonic-oscillator operators.[25] This is achieved by writing Eq. (5.2) in terms of the raising and lowering operators:

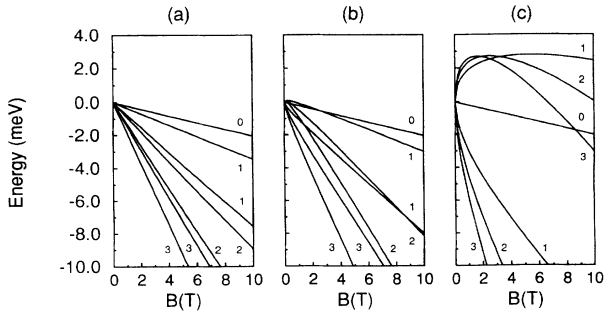

FIG. 3. Landau-level dispersion of the light-hole-derived states in the decoupled approximation, with (a) $C_4\varepsilon_{ax}=0.0$, (b) $C_4\varepsilon_{ax}=0.08$ eV Å (theoretical C_4), and (c) $C_4\varepsilon_{ax}=0.44$ eV Å (experimental C_4).

$$a^+=\frac{1}{\sqrt{2s}}(k_x+ik_y),\quad a^-=\frac{1}{\sqrt{2s}}(k_x-ik_y),\quad N=a^+a^-\ , \tag{5.5}$$

where $s=eB/\hbar c$. By inspection, the relevant harmonic-oscillator functions $u_n(x,y)$ for the 2×2 matrix (5.2) are

$$\begin{bmatrix} u_{n-1} & |-\frac{1}{2}\rangle \\ u_n & |+\frac{1}{2}\rangle \end{bmatrix}, \tag{5.6}$$

with n as the Landau-level quantum number. We then use the identities $a^+u_n=(n+1)^{1/2}u_{n+1}$, $a^-u_n=n^{1/2}u_{n-1}$, and $Nu_n=nu_n$ to give the Landau Hamiltonian, H_{Landau},

$$H_{\text{Landau}}=\begin{bmatrix} A_z+\hbar\omega_c(\gamma_1-\gamma_2-\kappa)/2 & -C_4\varepsilon_{ax}\sqrt{2sn} \\ -C_4\varepsilon_{ax}\sqrt{2sn} & A_z-\hbar\omega_c(\gamma_1-\gamma_2-\kappa)/2 \end{bmatrix}, \tag{5.7}$$

with

$$A_z=-\hbar\omega_c(\gamma_1-\gamma_2)n+E_{\text{LH}i}\ , \tag{5.8}$$

where ω_c is the cyclotron frequency eB/m_0c, $\kappa\approx1$,[15] and $E_{\text{LH}i}$ is the confinement energy of the ith light-hole state. The effect of C_4 is to produce a strong-coupling term between the $m_J=\pm\frac{1}{2}$ states. This term is proportional to $C_4\varepsilon_{ax}$, and thus will produce greater coupling for large C_4 values and strains. The resultant Landau dispersion for the first light-hole subband E_{LH1}, namely

$$E_n(B)=E_{\text{LH1}}-\hbar\omega_c(\gamma_1-\gamma_2)n \pm\tfrac{1}{2}\{8sn(C_4\varepsilon_{ax})^2+[\hbar\omega_c(\gamma_1-\gamma_2-\kappa)]^2\}^{1/2}\ , \tag{5.9}$$

is valid for $n\geq1$, while its negative-square-root solution is the only valid solution for $n=0$. Using parameters for GaAs,[15] the Landau levels are plotted against magnetic field in Fig. 3 with $n\leq3$ for (a) $C_4\varepsilon_{ax}=0.0$ eV Å, (b) $C_4\varepsilon_{ax}=0.08$ eV Å (moderate strain, theoretical C_4 value), and (c) $C_4\varepsilon_{ax}=0.44$ eV Å (large strain, experimental C_4 value). The average theoretical C_4 produces little difference from the Landau-level dispersion, while the large C_4 value will shift the dispersion significantly.

VI. CONCLUSION

We have used the empirical pseudopotential method and the tight-binding LCAO method to calculate the strain-induced linear-k (C_4) terms in the valence-band Hamiltonian of III-V semiconductors. The C_4 matrix elements calculated using the EPM are a factor of 3–4 smaller than the one experimental C_4 value available for InSb, as indicated in Table I, with the LCAO results lying between the EPM and the experimental value. We find that the C_4 terms have little effect on the valence-band dispersion near the valence-band maximum for layers under biaxial compression. The situation is more complicated for layers under biaxial tension, as little effect is found using the theoretically determined values of C_4, whereas the effects are becoming significant when we assume a value of C_4 equal to the one experimental value. We suggest that cyclotron-resonance measurements on p-doped layers under biaxial tension should confirm the magnitude of the C_4 terms and resolve the disagreement (by a factor of 4) between the calculated values of C_4 and the one experimental result to date on InSb.

In summary, the strain-induced linear-k terms are almost an order of magnitude larger than the linear-k terms due to inversion asymmetry in a quantum well under biaxial tension and lead to the highest valence subband being singly degenerate in all cases in such structures, with the valence-band maximum being shifted from the zone center. We suggest that further measurements are appropriate to quantify the magnitude of these effects.

ACKNOWLEDGMENTS

We thank U. Ekenberg for useful and stimulating discussions. This work was supported by the UK Science and Engineering Research Council.

[1]E. O. Kane, in *Semiconductors and Semimetals*, edited by R. K. Willardson (Academic, New York, 1966), Vol. 1, p. 75.
[2]M. Cardona, N. E. Christensen, and G. Fasol, Phys. Rev. Lett. **56**, 2831 (1986).
[3]D. A. Broido and L. J. Sham, Phys. Rev. **31**, 888 (1985).
[4]E. P. O'Reilly, Semicond. Sci. Technol. **4**, 121 (1989).
[5]H.-R. Trebin, U. Rössler, and R. Ranvaud, Phys. Rev. B **20**, 686 (1979).
[6]J. M. Luttinger and W. Kohn, Phys. Rev. **97**, 869 (1956).
[7]M. L. Cohen and T. K. Bergstresser, Phys. Rev. **141**, 789 (1966).
[8]W. A. Harrison, *Electronic Structure and the Properties of Solids* (Freeman, San Francisco, 1980).
[9]R. Sooryakumar and M. Cardona, *Solid State Commun.* **48**, 581 (1983).
[10]K.-R. Schulze, I. Topol, and E. Hess, Phys. Status Solidi B **55**, K75 (1973).
[11]E. Hess, I. Topol, K.-R. Schulze, H. Neumann, and K. Unger, Phys. Status Solidi B **55**, 187 (1973).
[12]J. P. Walter and M. L. Cohen, Phys. Rev. B **1**, 2661 (1970).
[13]D. J. Chadi, J. P. Walter, M. L. Cohen, Y. Petroff, and M. Balkanski, Phys. Rev. B **5**, 3058 (1972).

[14]T. K. Bergstresser and M. L. Cohen, Phys. Rev. **164**, 1069 (1967).
[15]*Physics of Group IV Elements and III-V Compounds,* edited by O. Madelung, Landolt-Börnstein, New Series, Group III, Vol. 17, Pt. a (Springer, New York, 1982).
[16]R. Ranvaud *et al.*, Phys. Rev. B **20**, 701 (1979).
[17]P. J. A. Thijs, E. A. Montie, T. van Dogen, and C. W. T. Bulle-Lieuwma, J. Cryst. Growth **105**, 339 (1990).
[18]C. E. Zah *et al.*, Electron. Lett. **27**, 1414 (1991).
[19]W. Batty *et al.*, Semicond. Sci. Technol. **4**, 904 (1989).
[20]P. Lawaetz, Phys. Rev. B **4**, 3460 (1971).
[21]L. W. Molenkamp *et al.*, Phys. Rev. B **38**, 4314 (1988).
[22]C. G. Van de Walle, Phys. Rev. B **39**, 1871 (1989).
[23]J. M. Luttinger, Phys. Rev. **102**, 1030 (1956).
[24]U. Ekenberg and M. Altarelli, Phys. Rev. B **32**, 3712 (1985).
[25]K. Hess, D. Bimberg, N. O. Lipari, J. U. Fischbach, and M. Altarelli, in *Proceedings of the 13th International Conference on the Physics of Semiconductors, Rome, 1976,* edited by F. G. Fumi (North-Holland, Amsterdam, 1976), p. 142.